

Silver Nanoparticles, Synthesized using *Hyptis suaveolens* (L) Poit and their Antifungal Activity against *Candida* spp.

Selvaraj Malathi,^[a, b] Dhayalan Manikandan,^[c] Ramasami Nishanthi,^[d] Enthai Ganeshan Jagan,^[b, e] Savaas Umar Mohammed Riyaz,^[f] Perumal Palani,^{*,[a]} and Jesus Simal-Gandara^{*,[g]}

Silver nanoparticles (AgNPs), due to their interesting properties and many potential applications have attracted enormous interests in recent years. An attempt has been made in this present study to synthesize AgNPs through biological reduction of silver nitrate, with leaf extract of *Hyptis suaveolens* (L) Poit serving as a reducing agent. AgNPs formed were characterized with spectral (UV-Vis, XRD, FTIR) and electron microscopic investigations. Dispersed spherical nanosilver particles in the range of 2 nm–85 nm were observed through microscopic analysis and the crystalline nature was evidenced through XRD analyses. Anticandidal activity of biosynthesized

AgNPs was evaluated against two *Candida albicans* strains. The minimum inhibitory concentration (MIC) values for AgNPs against the two clinical strains were 0.27 ± 0.03 $\mu\text{g/ml}$ and 0.97 ± 0.13 $\mu\text{g/ml}$. AgNPs were found to be more effective than the amphotericin-B used as control against the strains of the test pathogens. Scanning electron microscopic (SEM) analyses of the *Candida* cells treated with AgNPs shows change in the surface morphology, suggesting cell wall disruption to be a potential mode of anticandidal activity. Based on our observations, AgNPs synthesized with leaf extract of *Hyptis suaveolens* could be potentially used in combating candidal infections.

Introduction

Invasive fungal diseases are important causes of morbidity and mortality. Highly host adaptive fungal commensals evolve into deadly pathogens under dysbiosis conditions leading to disease state.^[1] Disease burden of various species of *Candida* causing Candidiasis, *Aspergillus* leading to Aspergillosis, Zygomycetes members like *Mucor*, *Rhizopus*, *Rhizomucor* causing

mucormycosis have been well documented.^[2] While the antibiotic armour against these opportunistic pathogens is limited, evolution of drug resistant strains skyrockets their threat.^[3] Recently during the COVID associated hospitalizations, among the patients with fungal co-infection, *Candida* spp. were the most frequently isolated fungal pathogen. *Candida* spp., a dimorphic fungus present in the normal flora of the healthy people; thriving commensally on the skin and mucosal layers, turns out to be an opportunistic pathogen causing superficial and systemic infections,^[4] in the immune compromised hosts. COVID, HIV infection, and broad spectrum of antibiotic therapy have resulted in significant outburst of candidiasis.^[5,6] Various ranges of antibiotics are currently in use to treat the candidal infections viz polyenes (amphotericin B), triazoles (fluconazole, itraconazole, voriconazole, and posaconazole), and echinocandins (caspofungin, micafungin, and anidulafungin).^[7] However administration of these kind of antibiotics are associated with complications including toxicity and other adverse side-effects.^[8–11] Therefore it is very crucial to find newer molecules for the treatment of *Candida* infections without any adverse effect on the host cells.

The advent of nanotechnology has offered unique solutions to several pressing problems plaguing the mankind and offers great promise and hope in overcoming them.^[12] The hybrid of nanoscale technologies with biology generally termed as nanobiology covers a wide range of topics like synthesis, fabrication, characterization of nano-dimensional entities from biological sources and its application in the biological realms. Nanomaterials with unique physical and chemical properties have found its way into biological realms. Different types of nanomaterials like copper, zinc, titanium,^[13] silver, magnesium, gold^[14] and alginate^[15] had been reported to exhibit antimicrobial and cytotoxic potentials. Among them, AgNPs had been

- [a] Dr. S. Malathi, Prof. P. Palani
Centre for Advanced Studies in Botany, University of Madras, Guindy Campus, Chennai, India
E-mail: palani7@unom.ac.in
smalathibt@sankaracollege.edu.in
- [b] Dr. S. Malathi, Dr. E. G. Jagan
Department of Biotechnology, Sri Sankara Arts and Science College (Autonomous), Enathur, Kanchipuram
- [c] Dr. D. Manikandan
Small Molecules and Drug Discovery group, Chengdu Anticancer Bioscience, Tianfu International Biotown, Chengdu 610000, China
- [d] Dr. R. Nishanthi
Department of Biotechnology, College of Science and Humanities, SRMIST, Kattankulathur - 603 203, Tamilnadu, India
- [e] Dr. E. G. Jagan
Department of Molecular Microbiology, School of Biotechnology, Madurai Kamaraj University, Madurai -625021, India
- [f] Dr. S. U. M. Riyaz
PG & Research Department of Biotechnology, Islamiah College (Autonomous), Vaniyambadi - 635752, Tamilnadu, India
- [g] Prof. J. Simal-Gandara
Universidad de Vigo, Nutrition and Bromatology Group, Analytical Chemistry and Food Science Department, Faculty of Science, E-32004 Ourense, Spain
E-mail: jsimal@uvigo.es

© 2022 The Authors. ChemistrySelect published by Wiley-VCH GmbH. This is an open access article under the terms of the Creative Commons Attribution License, which permits use, distribution and reproduction in any medium, provided the original work is properly cited.

proved to be most effective antimicrobial agent against fungi, bacteria, viruses and other eukaryotic micro-organisms.^[16,17] In view of their importance, AgNPs have been chosen in this present study and its' efficacy against *Candida albicans* was evaluated.

Antimicrobial property of nanoparticles are mainly dependent on their size, shape, pH, ionic strength and capping agent.^[18] It has also been reported that the smaller-sized spherical AgNPs demonstrated higher antiseptic efficacy than that of triangular AgNPs, whereas larger spherical AgNPs were found less efficient in bactericidal action than triangle shaped AgNPs against bacterial strains.^[19] Some reports suggested that isotropic geometries such as spherical particles demonstrated high antibacterial effectiveness. They claim that large surface to volume ratio of spherical shapes, which provided the maximum reactivity to obtain the highest antibacterial activity.^[20,21] Nano silver has been demonstrated to be an effective and fast acting fungicide against broad spectrum of common fungi like *Aspergillus*, *Malassezia*, *Candida* and *Saccharomyces*.^[22,23]

The biological reduction (green synthesis) method has been one of the most effective, economical and rapid method for synthesizing metallic nanoparticles and had been used to synthesize AgNPs.^[24] The plant used in this present study, *Hyptis suaveolens* (L.) Poit belonging to the family Lamiaceae has been commonly known as vilayati tulsi and has been an ethnobotanically important medicinal plant. The plant has been considered as an obnoxious weed, distributed throughout the tropics and subtropics. Almost all parts of this plant are being used in traditional medicine to treat various diseases. The leaves of *H. suaveolens* have been utilized as a stimulant, carminative, sudorific, galactogogue and as a cure for parasitic cutaneous diseases.^[25] Crude leaf extract is also used as a relief to colic and stomach ache. Leaves and twigs are considered to be antispasmodic and used in antirheumatic and antisuiporific baths,^[26] anti-inflammatory, antifertility agents,^[27] and also applied as an antiseptic in burns, wounds, and various skin complaints. Hence this plant has been chosen for the present study and an attempt has been made for a rapid synthesize of AgNPs using aqueous leaf extracts of *H. suaveolens* and various operational parameters were evaluated for biosynthesis route. Anticandidal effect on two different strains of *C. albicans* viz 5314 and 10261 was evaluated. In addition topological changes made by AgNPs on the cell surface of the *Candida* were evaluated using FESEM.

Experimental Section

Chemicals

All the chemicals and reagents used in this study were of analytical grade. Antifungal drug such as amphotericin B was purchased from HiMedia (India). Silver nitrate was obtained from Sigma-Aldrich Chemicals. De-ionised water employed in the study was collected from Merck-Milli-DI® water purification system. Culture media such as yeast nitrogen base (YNB) and yeast extract peptone dextrose agar (YEPDA) were purchased from Difco Laboratories (Detroit, MI, USA) and HiMedia (India).

Sample collection and extraction

The healthy leaves of *H. suaveolens* were collected from the Maraimalai (Guindy) Campus of University of Madras, India. Aqueous extract of *H. suaveolens* was prepared from freshly collected leaves (10 g). They were surface cleaned with running tap water, followed by distilled water and boiled with 100 ml of distilled water at 100 °C for 15 min. This extract was filtered through Whatman filter paper No.1 and used for further experiments.

Synthesis of silver nanoparticles

For synthesis of AgNPs, 3 ml of AgNO₃ (1 mM) solution was added with the aqueous extract of *H. suaveolens* and incubated in dark (to prevent the photo activation of silver nitrate) under static conditions.^[28] The reaction conditions were optimised for the concentrations of the plant extract, kinetics of contact time, temperature and different concentration of metal ion. A control setup was also maintained without the extract throughout the conduct of the experiment.

Characterization studies

The reduction of silver ions was monitored using UV/Vis double beam spectrophotometer (HITACHI 2900, Japan) by scanning an aliquot of the reactant mixture at a wavelength range of 300 to 700 nm. The size, shape and composition of the nanoparticles were analysed using TEM (JEOL-JEM-2100, Japan) equipped with EDX, DLS(Zetasizer Nano ZS, Malvern Instruments Ltd., UK), XRD (Philips, USA), and FT-IR (Perkin Elmer, Germany) studies. For TEM analysis, the nanosol was filtered through 0.2 micron sterile filter to remove the impurities if any. Samples for TEM studies were prepared by placing 3 µl of the nanosol filtrate on the carbon coated copper grid, making a thin film of sample on the grid. The excess sample was removed using the cone of a blotting paper and kept in grid box sequentially. For XRD and FTIR analysis, AgNPs were pelleted out of the nanosol by centrifugation process at 10,000 rpm for 15 min, air dried and used. The purity of the AgNPs were analysed by subjecting the sample to XRD studies using Philips X-Ray Diffractometer with Philips PW 1830 X-Ray Generator operated at a voltage of 40 kV and a current of 30 mA with Cu Kα1 radiation. Further, functional groups of the stabilising and capping molecules adherent onto the AgNPs surface were determined through FT-IR analysis by KBr (FTIR grade) pellet method.

Anti-candidal activity by disc diffusion method

Anti-candidal activity was evaluated against two different clinical strains of *Candida albicans* 5314 and 10261. The AgNPs synthesized using *H. suaveolens* plant extract were tested for their antimicrobial activity by disc diffusion method. The pure cultures of the test organisms were sub-cultured in YNB broth at 35 °C and kept on rotary shaker at 200 rpm. The Muller Hinton agar plates (MHA) were swabbed with the 18–24 h old fungal pathogens to create a confluent lawn of fungal growth (1 × 10⁵ cells /ml). Paper disc of 6 mm dimension (Hi-Media, India) was impregnated with 25 µl silver nanoparticles. Amphotericin B (10.24 mg/10 mL) used as positive control. Efficacy of plant extract and silver nitrate was also compared. The discs were gently pressed to get better contact with Muller Hinton Agar. The plates were incubated for 24 h at 37 °C. After incubation at 37 °C, the different levels of zone of inhibition were measured. After incubation the susceptibility of the test

organisms was determined by measuring the diameter of the zone of inhibition.

Minimal inhibitory concentration of silver nanoparticles

The determination of MIC of the AgNPs against *C. albicans* was performed as per the recommendations of the Clinical Laboratory Standard Institute.^[29] The yeast cells of *C. albicans* were grown planktonically under aerobic conditions at 37 °C for 24 h in YNB broth. The cell count was made with hemocytometer, and a standardized cell suspension (1×10^5 cells/ml) was prepared. One hundred microliters of the cell suspension was dispensed in triplicate microtiter wells to which 100 μ l suspension containing different concentrations of nanoparticles in YNB medium was added and mixed well. Conventionally used antifungal agent such as amphotericin B^[30] was used in order to compare the antifungal potential of AgNPs. Amphotericin B was dissolved in dimethyl sulfoxide (DMSO) and diluted with sterile YNB medium to obtain drug concentrations ranging from 0.0313 to 1024 μ g/ml. The cells with either nanoparticles or conventionally used antifungal were incubated at room temperature for 24 h, and the growth inhibition was measured spectrophotometrically at 600 nm (Powerserve XS Biotech, USA). Wells with cells without AgNPs were used as the

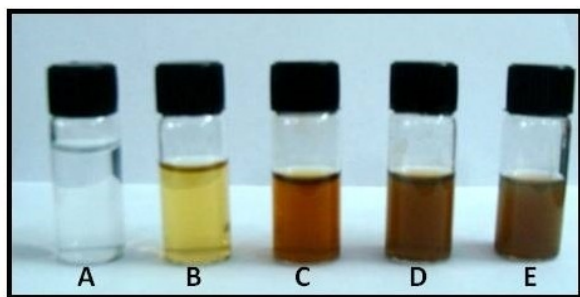


Figure 1. Formation of AgNPs as visualized by visible color change. A- Silver Nitrate; B -Plant Extract; C - 1:60 V/V; D - 1:30 V/V; E - 1:20 V/V.

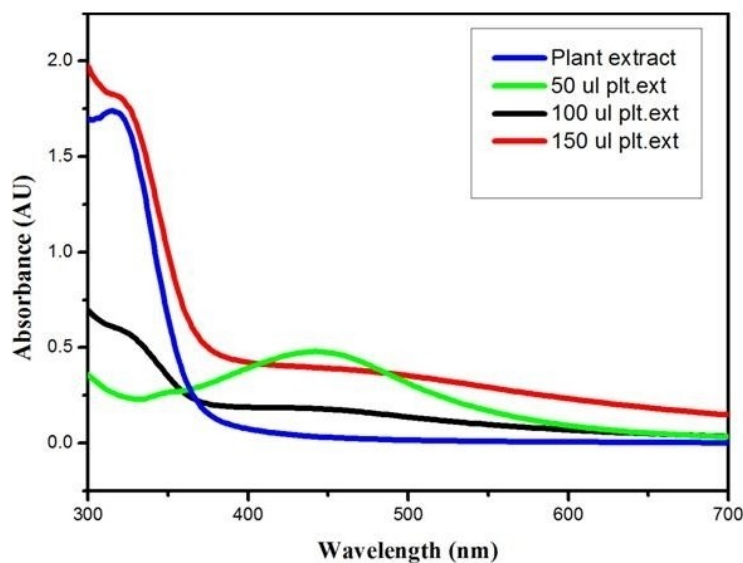


Figure 2. UV-Vis spectra of AgNPs synthesized with different concentrations of *H. souveolens* leaf extract.

Table 1. Antimicrobial activity of AgNPs and antifungal drug against *Candida albicans*.

Test Compounds	Zone of inhibition (mm)	
	<i>Candida albicans</i> 10261	<i>Candida albicans</i> 5314
Silver nanoparticles	22 ± 0.43	20 ± 0.75
Amphotericin B	18 ± 0.5	18 ± 0.6
Silver nitrate	16 ± 0.43	15 ± 0.45
Plant extract	[NZI]	[NZI]

[Data are represented as mean ± standard deviation; NZI – No zone of inhibition]

control. The MIC was calculated as the lowest amount of AgNPs that inhibited 50% growth of *C. albicans* cells under the experimental conditions.

Scanning electron microscopy (SEM)

One millilitre of candidal suspension (1×10^5 cells/ml) was incubated with AgNPs at their MIC values for 24 h and observed in FESEM (H-7650, Hitachi, Japan), and the morphological changes were observed. The cells grown on YNB medium without AgNPs served as the control.

Results and Discussion

Synthesis of silver nanoparticles

The reduction of silver ions (Ag^+) in aqueous extract of *H. souveolens* was marked by a visible colour change (colourless to reddish brown) of the reaction mixture (Figure 1). The aqueous leaf extract reduced the Ag^+ and lead to the formation of silver hydrosol. The control AgNO_3 solution (without extract) showed no change of colour.

The synthesis of AgNPs in the reaction mixture was monitored using UV-Visible spectroscopy. AgNPs synthesized

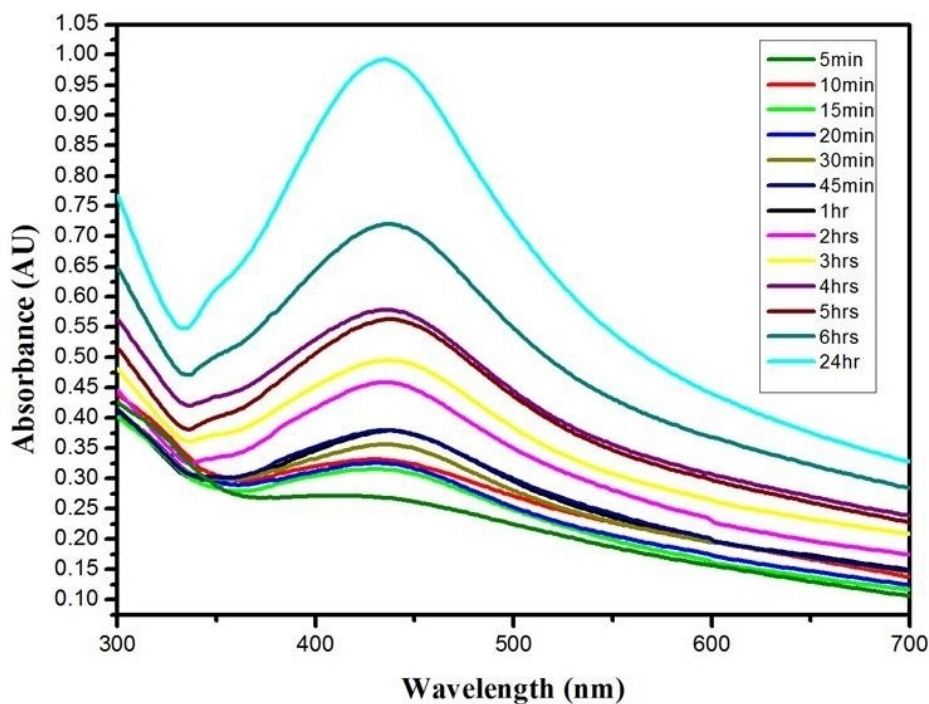


Figure 3. UV-Vis spectra of AgNPs synthesised with *H. souveolens* leaf extract at kinetics of contact time.

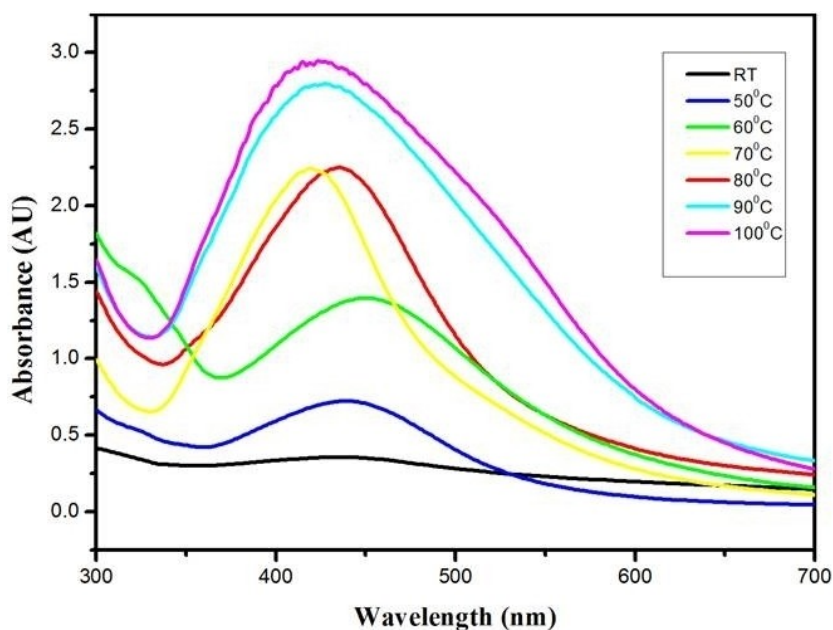


Figure 4. UV-Vis spectra of AgNPs synthesised with *H. souveolens* leaf extract at different temperatures.

were evident by the occurrence of a characteristic Surface Plasmon Resonance (SPR) peak at 435 nm. SPR patterns, characteristics of metal nanoparticles are strongly dependent on the particle size, stabilizing molecules or the surface adsorbed particles and the dielectric constant of the medium.^[31] SPR plays a major role in the determination of

optical absorption spectra of metal nanoparticles, which shifts to a longer wavelength with increase in the particles size.^[32]

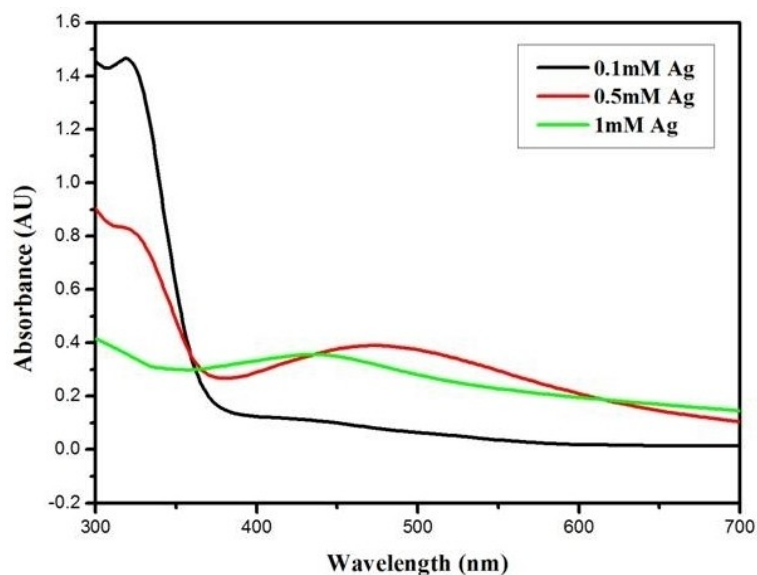


Figure 5. UV-Vis spectra of AgNPs synthesised with *H. souveolens* leaf extract at different concentration of metal ion.

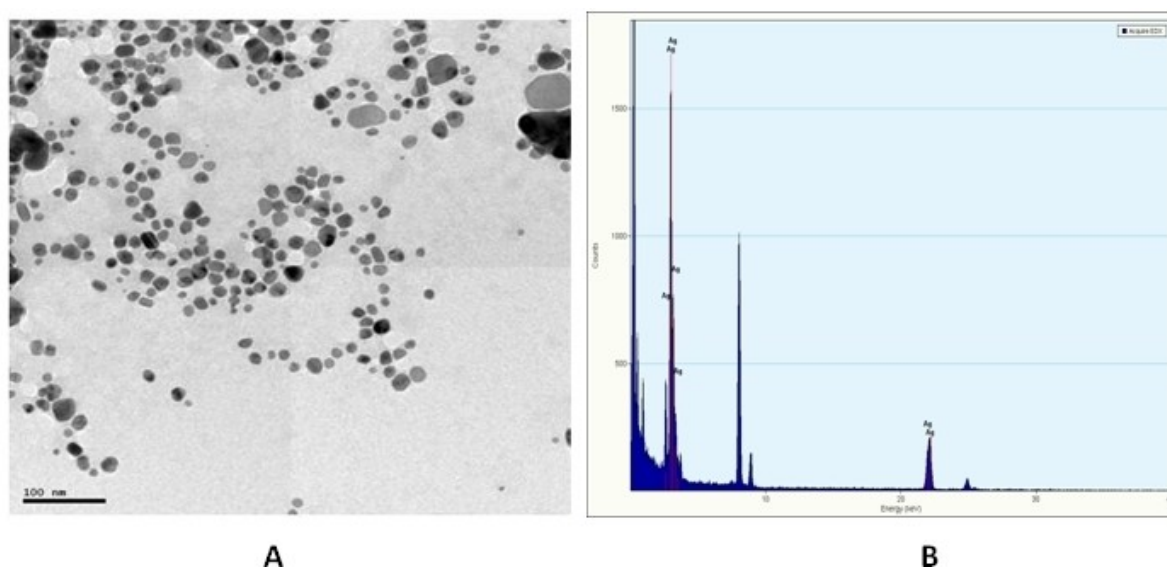


Figure 6. A-Transmission electron microscopic image of the synthesised AgNPs. B - EDAX spectrum showing the peak for silver.

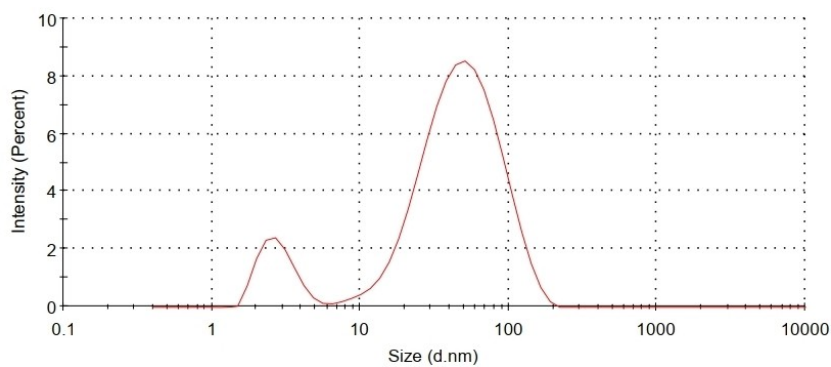


Figure 7. DLS spectrum of AgNPs synthesised using the leaf extract of *H. souveolens*.

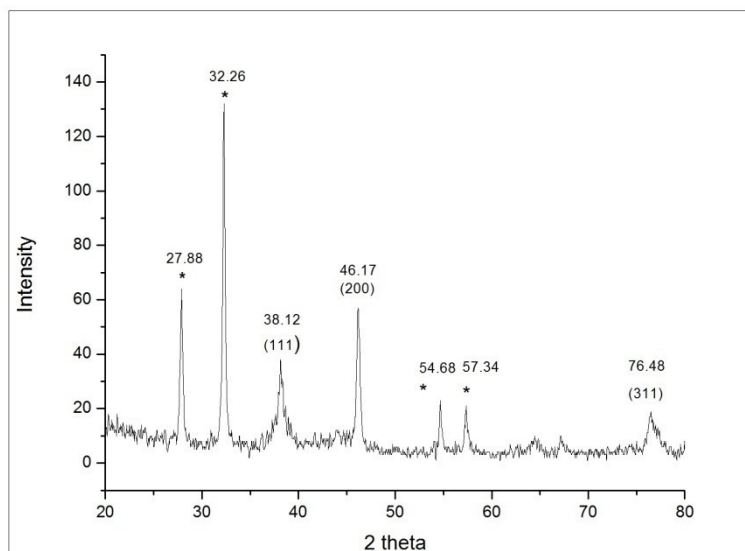


Figure 8. XRD pattern of AgNPs synthesized from the leaf extract of *H. suaveolens*.

Optimization of AgNPs synthesis using different parameters

The reaction parameters such as concentrations of leaf extract, silver nitrate solution, reaction time and temperature were optimized through one factor at a time (OFAT) approach.

Effect of different concentrations of leaf extract

The concentration of leaf extract to silver nitrate (1 mM) solution in the reaction mixture was varied in the range of 1:60, 1:30 and 1:20 V/V at 37 °C. UV-Visible spectrum analysis revealed that leaf extract and silver nitrate solution at 1:60 V/V concentrations was effective over the other tested concentrations, which was evident from the sharper SPR peak at 435 nm. The intensity of the absorption spectra recorded for other test concentration of leaf extract was smaller and it may be due to decreased or low synthesis of silver nanoparticles. A control setup with no silver nitrate solution (leaf extract alone) did not show any peak in the absorption region specific for silver (Figure 2). Furthermore, higher concentration of leaf extracts had been attributed with enhanced agglomeration of nanomaterials.^[33] Hence, leaf extract at 1:60 V/V dilutions has been considered to be optimal for AgNP synthesis.

Effect of contact time on AgNPs synthesis

A visible change in the colour of the reaction mixture from yellow to bright red and then to dark brown was observed during the incubation. The rate of AgNPs formation in the reaction mixture was followed over 24 h period and occurrence of AgNPs specific peaks started within 5 min, whose intensity increased up to 24 h. The spectrum in Figure 3 clearly shows that as the time increases, the intensity of the peak at 435 nm corresponding to the SPR of AgNPs increased. There was no change in the spectra even after 24 h which indicates that the

reaction came to equilibrium at 24 h. Interestingly the solution was extremely stable even after 24 h, with no evidence of aggregation of particles. These observations corroborated with the previous report^[34] on *H. suaveolens* dried leaf extract based reduction of silver and stabilization of AgNPs. Previously, rapid synthesis of AgNPs with *Boswellia ovalifoliolata* plant extract was reported in 10 minutes and *Shorea tumbuggaia* plant extract took 15 min.^[35] AgNPs were formed within 30 min using the leaf extracts of *Acalypha indica* as a reducing agent.^[28]

Effect of temperature on the synthesis of AgNPs

In an attempt to optimize the temperature for optimal synthesis of AgNPs, the SPR peak and its intensity were found to shift towards higher wavelength and increase respectively with an increase in the reaction temperature (Figure 4). The phenomenon could be attributed to enhanced conversion of metal ions to nanoparticles at elevated temperatures. While the trend observed in this study corroborates with several earlier reports, optimum temperature for AgNPs synthesis through bio-reduction methods had been reported around 37 °C.^[36,37] Agglomeration of AgNPs had been reported at elevated reaction temperature,^[36] however in this study we confirmed the stability of AgNPs even at higher temperatures. There was no agglomeration even at 100 °C. Among the various temperature tested, 70 °C was found to be the most optimum for the silver nanoparticles, as it shows absorption peak at 421 nm.

Effect of different concentrations of silver metal ion

Concentration of silver nitrate plays a major role in the nanoparticle synthesis. Different concentrations of silver ions were evaluated by maintaining other parameters at optimised levels for the synthesis of AgNPs. Colour intensity increases with the increase in silver nitrate concentrations at a fixed

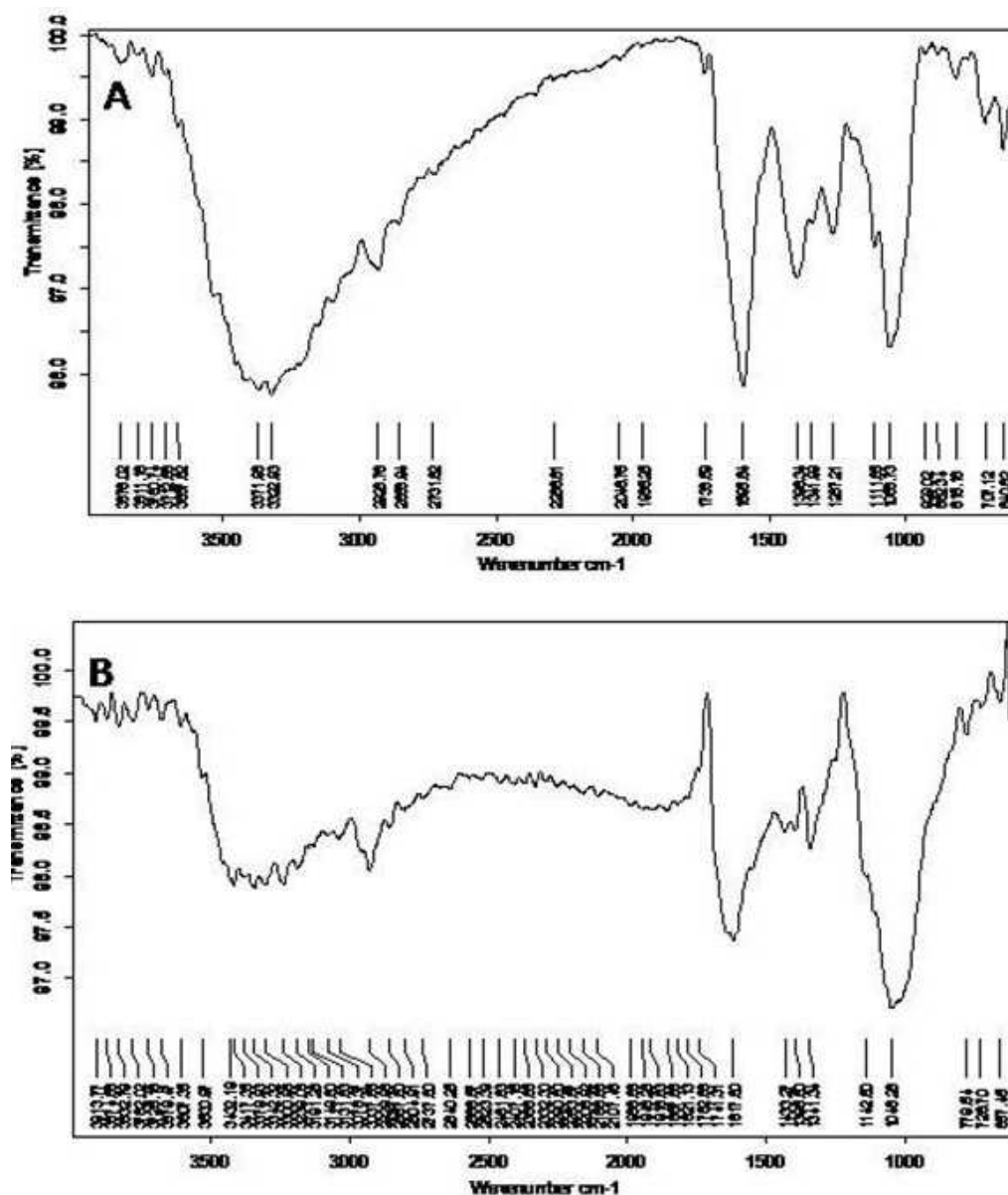


Figure 9. FTIR spectrum of aqueous leaf extract of *Hyptis suaveolens* (A) and AgNPs synthesized by reduction of Ag⁺ ions by leaf extract (B).

volume fraction of leaf extract. Among the various concentrations tested 1 mM of AgNO₃ was found to be the optimum for synthesis of AgNPs and this is in good agreement with the earlier reports.^[38] At 0.5 mM of AgNO₃, occurrence of larger grain or agglomerates resulted in the peak shift to a higher wavelength, thereby making it unsuitable for the synthesis purposes (Figure 5). They also reported that increasing concentrations of AgNO₃ increased the agglomeration of Ag⁺ to AgNPs. The synthesis of AgNPs was found to be low at low metal ion (0.1 mM AgNO₃) concentration and hence absorbance was also weaker.

Transmission electron microscopy (TEM) and EDAX

The size and morphology of the nanoparticles were analysed with a Transmission Electron Microscope (TEM). The TEM micrograph (Figure 6) shows well-dispersed particles that are more or less spherical, one or more aggregated as well as faceted particles. The polydispersed nanoparticle ranged between 2 nm to 85 nm. Similar results had been documented in several plant extract based AgNPs synthesis.^[24,39] Recently AgNPs ranging about 29.5 nm to 52.27 nm were synthesised using the dried leaves extract of *H. suaveolens*.^[34] Size of the AgNPs synthesized using *Cyprus pangorei* extracts ranged about 32–60 nm^[40] and with *Cycas* leaf extracts ranged about 2–6 nm.^[41]

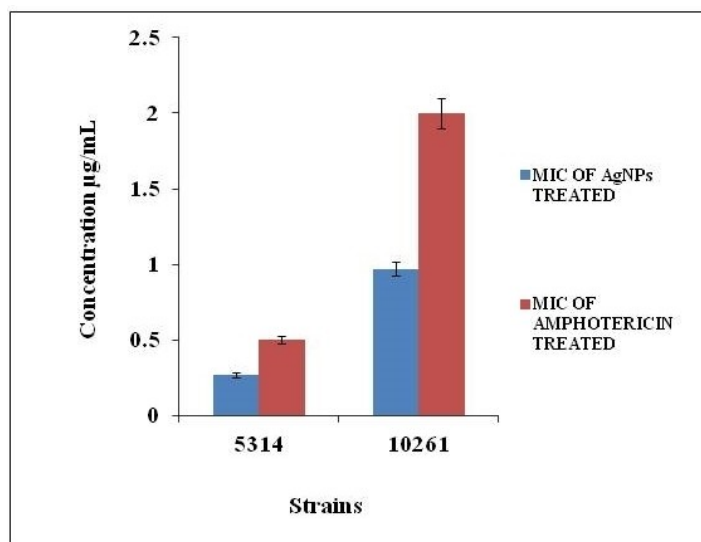


Figure 10. Minimal inhibitory concentration of AgNPs against *Candida albicans* 5314 and *Candida albicans* 10261.

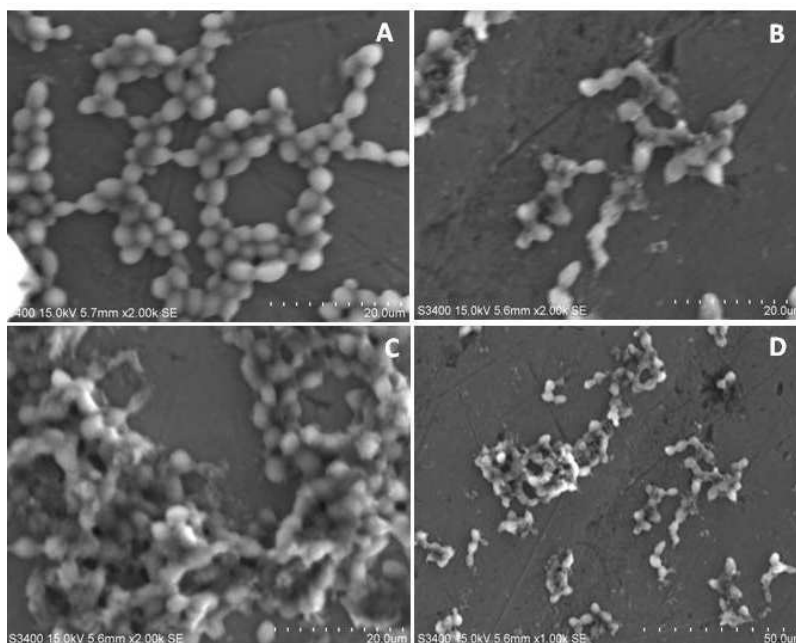


Figure 11. Surface topography of *Candida albicans* 5314 control (A); treated with AgNPs (B,C,D).

Most studies had reported formation of spherical AgNPs,^[24,39] although other forms were sparsely reported. Spherical, triangular, square, oval shaped AgNPs were synthesised using Corn cobs xylan,^[42] while spherical and cuboidal AgNPs were synthesised from leaf extracts of *Citrus medica*.^[43] In biological synthesis methods, exercising strict control over the size and shape of the nanoparticles has been elusive,^[24,44] understanding the impact of individual process variables and their interactions would be the key towards achieving it. The purity of the biosynthesised AgNPs were investigated through EDX analysis. AgNPs generally shows a typically strong signal

peak at 3 KeV, due to surface plasmon resonance.^[45] In the present investigation, strong signals for Ag from the synthesised AgNP were observed at 3–4 KeV. Similar results were reported for AgNPs synthesised with varied sources of bioreactants.^[45,46]

Dynamic light scattering

The size distribution pattern of AgNPs was determined by monitoring the dynamic fluctuations in the light scattering intensity of the particles. Two major population based on size

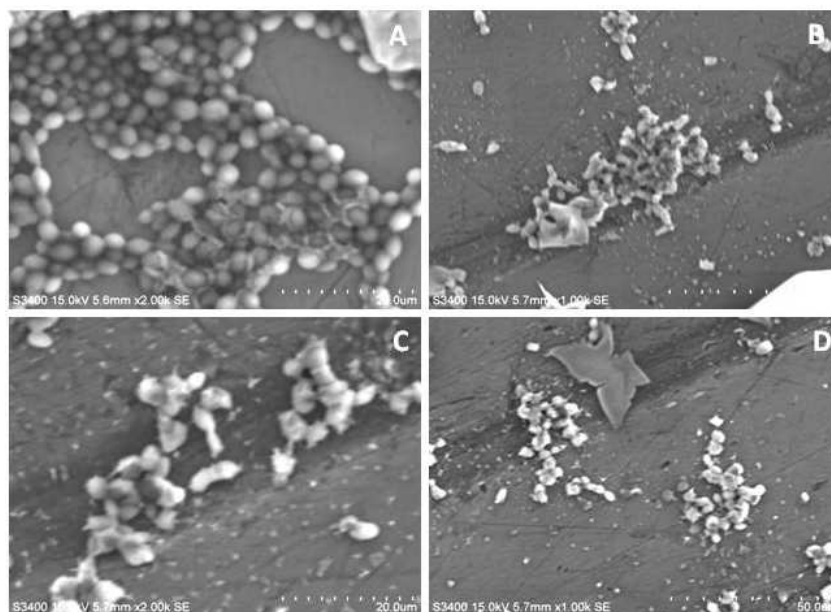


Figure 12. Surface topography of *Candida albicans* 10261 control (A); treated with AgNPs (B,C,D).

could be discerned whose average ranged about 2.8 ± 0.87 nm and 54.75 ± 31.24 nm (Figure 7). These size measurements corroborated with the results obtained in TEM analysis (2–85 nm). Further the DLS measurements confirmed the stable hydrodynamic properties of the AgNPs.

X-ray diffraction was carried out to confirm the crystalline nature of the particles. XRD analysis showed four distinct diffraction peaks at 38.12° , 46.17° , and 76.48° corresponding to the planes (111), (200), and (311) of the cubic face-centered silver (Figure 8). The unassigned peaks at 27.88° , 32.26° , 54.68° and 57.34° were due to the crystallization of bioorganic phases that occur on the surface of NPs.^[47,48] The lattice constant calculated from this diffraction pattern was 4.08 \AA and the data obtained matched with that in the database of Joint Committee on Powder Diffraction Standards (JCPDS), file No. 01-1167. The average grain size of the AgNPs formed in the bioreduction process was determined using Scherrer's formula, $d = 0.9\lambda / B \cos\theta$ and was estimated as 35 nm. The XRD pattern thus clearly showed that the crystalline nature of AgNPs formed in this study and corroborated with the previous studies.^[48,49]

Fourier transformed infrared spectroscopy (FTIR)

The biosynthesised AgNPs and the lyophilized leaf extract of *H. suaveolens* were characterized using Fourier Transformed Infrared Spectroscopy (FTIR) by scanning them in the range $450\text{--}4000 \text{ cm}^{-1}$ at resolution of 4 cm^{-1} . FTIR analysis was carried out to identify the bio molecules responsible for the reduction of silver ions and functional groups adherent onto the surface of the AgNPs. In FTIR spectrum (Figure 9) of the leaf extract of *H. suaveolens* the peak stretching extending at 3371.98 cm^{-1} and 3322.93 cm^{-1} were of free NH and H-NH group respectively. Reduction in the intensity of these peaks was observed in

AgNPs suggesting formation of amide linkages. Peaks at 3667.82 and above denoted the presence of free OH groups. Peaks in the range of $3000\text{--}3300 \text{ cm}^{-1}$ are characteristics of OH stretching from carboxylic acids. Peak at 1736.59 cm^{-1} , 1267.21 cm^{-1} and 1058.73 cm^{-1} corresponded to C=O, aliphatic ester and aliphatic ether vibrations respectively. Their intensities also increased significantly in AgNPs suggesting occurrence of condensation reactions to stabilizing the nanoparticles. Similarly, the peak at 1341.99 cm^{-1} and 1396.34 cm^{-1} in the leaf extract corresponded to aromatic amine and S=O group respectively were significantly reduced in the IR spectrum of AgNPs. The peak at 1595.84 cm^{-1} in the leaf extract corresponds to the nitro compound was lacking in the IR spectra of AgNPs. Multiple weak peaks pertaining to C=C stretching in the range of $2100\text{--}2260 \text{ cm}^{-1}$ and CH stretchings in the range of $2840\text{--}3000 \text{ cm}^{-1}$ were observed to be more pronounced in the IR spectrum of AgNPs. The strong affinity of the amide group of proteins towards the metal and its contribution to the stability of the nanoparticles was reported erstwhile.^[49] Detailed reviews of the plant based synthesis of AgNPs have established that the metabolites in the plant extracts contribute to the reduction and stabilization process. Our results suggest that the surface of the AgNPs were harbouring plant based biomolecules and it could confer stability to AgNPs. The extracts of *H. suaveolens* had been earlier reported to harbour phytochemicals like essential oils, tannins, saponins, phenols, flavonoids, terpenoids, alkaloids, and sterols.^[50] They have served as the source of biomolecules in this study.

Anticandidal activity

The anticandidal activity of AgNPs was investigated against two different strains of *Candida albicans* 5314 and 10261 using disc diffusion technique. Amphotericin B was used as reference drug. The antifungal activity of the phytosynthesized AgNPs showed higher inhibitory activity than the standard drug. The results clearly depicts that the efficiency of the AgNPs is better than the conventionally used drug. The inhibitory zone produced by the AgNPs against the *C. albicans* strains 5314 was found to be 20 mm and 10261 were 22 mm (Table 1); on par with commercial drug and higher than silver nitrate. The AgNPs synthesized from leaf extract of *Lotus lalambensis* Schweinf exhibited about 24 mm ZI against *C. albicans*.^[51] AgNPs (20–45 nm) synthesized using *Streptomyces* sp.VITPK1 exhibited about 20 mm ZI against *C. albicans*, *C. tropicalis* and *C. krusei*.^[52]

Determination of Minimal Inhibitory Concentration

Minimum inhibitory concentration (MIC) test was performed to check the minimum concentration of biogenic AgNPs against *Candida* strains. MIC test reveals the existence of antifungal activity at different concentration levels. In this present investigation the MIC test value of biogenic AgNPs against both the strains of *Candida albicans* 5314 and 10261 was calculated as 0.27 ± 0.03 $\mu\text{g/ml}$ and 0.97 ± 0.13 $\mu\text{g/ml}$ respectively and Amphotericin B was calculated as 0.5 $\mu\text{g/mL}$ and 2 $\mu\text{g/mL}$ respectively (Figure 10). Interestingly it was found that the IC_{50} value was very much lower than the IC_{50} value of the commercial drug. AgNPs produced using different plant extracts found to be effective against *Candida* sp. AgNPs biosynthesized by the *Calotropis gigantea* leaf extract against *C. albicans* with an MIC of 50 $\mu\text{g/mL}$.^[53] AgNPs synthesized using the extract of *Lycopersicon esculentum* displayed inhibitory action against *C. albicans*, *C. parapsilosis*, and *C. glabrata* with an MIC of 8 $\mu\text{g/mL}$ while biosynthesized AgNPs using *Artemisia annua* showed MIC against *C. albicans*, *C. tropicalis*, and *C. glabrata* that ranged between 80 and 120 $\mu\text{g/mL}$.^[54] Thus, AgNPs produced by different approaches and species were reported to show antifungal activity at different MIC levels depending on their size, shape, and surface modification.^[51,55] Size of the nanoparticles plays an important role in the antimicrobial property. It had been reported that the size and shape of the metallic nanoparticles influence their chemical, optical and thermal properties. In our previous report we have reported that PVP-stabilized quantum sized AgNPs work as a potent antifungal agent at very low concentration. The MIC value obtained was very much lower when compared with other known antifungals.^[17]

Scanning Electron Microscopy

SEM images reveal that the cell morphology of the AgNPs treated and untreated *Candida* cells differ widely. The clear budding of the cells can be observed in untreated cells whereas in AgNPs treated cells no such budding was observed. Cell shrinkage was observed in treated cells due to the cell

leakage (Figure 11 & 12). AgNPs treatment could have created pores on the cell wall and penetrated into the cells which might have caused the cell damage. Previous reports suggests that the AgNPs entering into the cells reacts with the microbial enzymes and release reactive oxygen species, leading to the membrane damage and cell destruction.^[56] It had also been reported that disruption of membrane morphology may cause a significant increase in permeability, leading to uncontrolled transport through the plasma membrane and finally cell death.^[57] Recent reports confirms that AgNPs creates pores on the cell wall which leads to the leakage of ions which causes the membrane lipid bilayer damage.^[51] Different mechanisms have been proposed on mode of action of silver nanoparticles. Silver has greater tendency towards sulphur or phosphorous containing bases. Hence sulphur containing proteins in the membrane or inside the cells and phosphorous containing elements like DNA are the preferential sites for AgNPs binding.^[58,59] AgNPs block the cell cycle at G2/M phase in *C. albicans* which results in the production of reactive oxygen species (ROS) and decreases the metal based antioxidant enzymes.^[60,61]

Conclusion

The present work identifies an ethanobotanically valuable plant, *Hyptis suaveolens* (L) Poit as a source of bio-reductant and stabilizing agent for AgNPs synthesis in environmentally benign and economically viable route. The spherical AgNPs synthesised exhibited no agglomeration over the study period and manifested well pronounced anticandidal effects. The MICs recorded against *Candida albicans* strains were significantly better than Amphotericin B, suggesting that they could be a formulated into anticandidal preparations after a serious of *in vivo* and toxicity studies. Pharmaceutical preparations with AgNPs alone or in conjugation with conventional antifungal therapeutics could also be generated to effectively combat candidiasis and other mycoses in immuno-compromised individuals.

CRedit authorship contribution statement

Malathi Selvaraj – Conceptualization, Methodology, Investigation, Writing - original draft. Nishanthi Ramasami – Sample preparation, execution. Enthai Ganeshan Jagan - Writing the manuscript. Dhayalan Manikandan – Data curation. Savaas Umar Mohammed Riyaz – Formal analysis. Perumal Palani – Supervision, reviewing and editing. Jesus Simal-Gandara–Conceptualization, Reviewing and editing.

Acknowledgements

The authors SM, RN and PP acknowledge The Director, Centre for Advanced Studies in Botany for providing laboratory facilities. Funding for open access charge: Universidade de Vigo/CISUG.

Conflict of Interest

The authors declare no conflict of interest.

Data Availability Statement

The data that support the findings of this study are available from the corresponding author upon reasonable request.

Keywords: AgNPs - Silver nanoparticles · *Candida albicans* · TEM · *Hyptis suaveolens* L

- [1] J. J. Limon, J. H. Skalski, D. M. Underhill, *Cell Host Microbe*. **2017**, *9*, 156–165.
- [2] M. Hoenigl, D. Seidel, R. Sprute, C. Cunha, M. Oliverio, G. H. Goldman, A. S. Ibrahim, A. Carvalho, *Nat Microbiol*. **2022**, *7*, 1127–1140.
- [3] M. C. Fisher, A. Alastruey-Izquierdo, J. Berman, et al. *Nat. Rev. Microbiol*. **2022**, *20*, 557–571.
- [4] M. S. Lionakis, M. G. Netea, *PLoS Pathog*. **2013**, *9*, e1003079.
- [5] Y. Jin, L. P. Samaranyake, Y. Samaranyake, H. K. Yip, *Arch. Oral Biol*. **2004**, *49*, 789–798.
- [6] M. Henriques, S. Silva, *Microorganisms*. **2021**, *9*, 704.
- [7] A. R. Padmavathi, P. Murthy, A. Das, A. Priya, T. J. Sushmitha, S. Karutha Pandian, S. R. Toleti, *Biofouling*. **2020**, *36*, 56–72.
- [8] M. D. Levin, J. G. D. Hollander, B. Van der Holt, B. J. Rijnders, M. V. Vliet, P. Sonneveld, R. H. N. Van Schaik, *J. Antimicrob. Chemother*. **2007**, *60*, 1104–1107.
- [9] C. Taxvig, U. Hass, M. Axelstad, M. Dalgaard, J. Boberg, H. R. Andeasen, A. M. Vinggaard, *Toxicol. Sci*. **2007**, *100*, 464–473.
- [10] L. J. Worth, C. C. Blyth, D. L. Booth, D. C. Kong, D. Marriott, M. Cassumbhoy, J. Ray, M. A. Slavin, J. R. Wilkes, *Intern. Med. J*. **2008**, *38*, 521–537.
- [11] K. Venkatakrishnan, L. L. VonMoltke, D. J. Greenblatt, *Clin. Pharmacokinetics*. **2000**, *38*, 111–180.
- [12] M. A. Albrecht, C. W. Evan, C. L. Raston, *Green Chem*. **2006**, *8*, 417–32.
- [13] P. S. Retchkiman-Schabes, G. Canizal, R. Becerra-Herrera, C. Zorrilla, H. B. Liu, J. A. Ascencio, *Opt. Mater*. **2006**, *29*, 95–9.
- [14] H. Gu, P. L. Ho, E. Tong, L. Wang, B. Xu, *Nano Lett*. **2003**, *3*, 1261–3.
- [15] Z. Ahmad, R. Pandey, S. Sharma, G. K. Khuller, *Ind J Chest Dis Allied Sci*. **2005**, *48*, 171–6.
- [16] P. Gong, H. Li, X. He, K. Wang, J. Hu, W. Tan, W. Tan, S. Zhang, S. Yang, *Nanotechnology*. **2007**, *18*, 604–11.
- [17] M. Selvaraj, P. Pandurangan, N. Ramasami, S. B. Rajendran, S. N. Sangilimuthu, P. Perumal, *Appl. Biochem. Biotechnol*. **2014**, *173*, 55–66.
- [18] S. Ahmed, M. Ahmad, B. L. Swami, S. Ikram, *J. Adv. Res*. **2016**, *7*, 17–28.
- [19] M. A. Raza, Z. Kanwal, A. Rauf, A. Nasim Sabri, S. Riaz, S. Naseem, *Nanomaterials*. **2016**, *6*, 74.
- [20] S. Agnihotri, S. Mukherji, S. Mukherji, *RSC Adv*. **2014**, *4*, 3974–3983.
- [21] A. A. El-Kheshen, S. F. G. El-Rab, *PharmaChem* **2012**, *4*, 53–65.
- [22] J. E. Mussin, M. V. Roldán, F. Rojas, et al. *AMB Expr*. **2019**, *9*, 131.
- [23] H. Yu, M. Chen, P. M. Rice, S. X. Wang, R. L. White, S. Sun, *Nano Lett*. **2005**, *5*, 379–82.
- [24] D. Bamal, A. Singh, G. Chaudhary, M. Kumar, M. Singh, N. Rani, P. Mundlia, A. R. Sehwat, *Nanomaterials*. **2021**, *11*, 2086.
- [25] The Wealth of India: A Dictionary of Indian Raw Materials and Industrial Products (Industrial Products-Part I) *Ind Med Gaz*. **1949**, *84*: 476–7.
- [26] K. R. Kirtikar, B. D. Basu, *Indian Medicinal Plants* **1935**, Vol. II. Lalit Mohan Publication, Allahabad, 1347–1348.
- [27] S. Mahesh, **2001**, *Antiseptic use of H. suaveolens*, Publication No: G138. Tropical product Institute. UK.
- [28] C. Krishnaraj, E. G. Jagan, S. Rajasekar, P. Selvakumar, P. T. Kalaichelvan, N. Mohan, *Colloids Surf. B*. **2010**, *76*, 50–56.
- [29] CLSI. **2008**, Reference method for broth dilution antifungal susceptibility testing of filamentous fungi; approved standard CLSI document M38-A2. Wayne: Clinical and Laboratory Standards Institute.
- [30] S. Hartsel, J. Bolard, *Trends Pharmacol. Sci*. **1996**, *17*, 445–9.
- [31] K. B. Mogensen, K. Kneipp, *J. Phys. Chem. C*. **2014**, *118*, 28075–28083.
- [32] A. R. V. Nestor, V. Sanchez-Mendieta, M. A. Camacho-Lopez, R. M. Gomez-Espinosa, M. A. Camacho-Lopez, J. A. Arenas-Alatorre, *Mater. Lett*. **2008**, *62*, 3103–3105.
- [33] P. V. Parashar, R. Parashar, B. Sharma, A. Pandey, *Dig. J. Nanomater. Biostructures*. **2009**, *4*, 45–50.
- [34] B. Lateef, S. M. Oladejo, P. O. Akinola, D. A. Aina, L. S. Beukes, B. I. Folarin, E. B. Gueguim-Kana, *Mater. Sci. Eng. 2020, IOP Conf. Ser.* **2020**, *805*, 012042.
- [35] N. Savithramma, M. Linga Rao, K. Rukmini, P. Suvarnalatha Devi, *Int. J. Chem. Tech. Res*. **2011**, *3*, 1394–1402.
- [36] P. Balashanmugam, M. D. Balakumaran, R. Murugan, K. Dhanapal, P. T. Kalaichelvan, *Microbiol. Res*. **2016**, *192*, 52–64.
- [37] A. D. Dwivedi, K. Gopal, *Colloids Surf. A*. **2010**, *369*, 27–33.
- [38] R. G. Kumar, S. Raman, R. Praveen, S. S. Kumar, *Green Processing and Synthesis*. **2019**, *8*, 144–156.
- [39] M. Chung, I. Park, K. Seung-Hyun, M. Thiruvengadam, G. Rajakumar, *Nanoscale Res. Lett*. **2016**, *11*, 40.
- [40] C. Parvathiraja, S. Shailajha, S. Shanavas, Gurung, *J. Appl. Nanosci*. **2020**, *11*, 477–491.
- [41] A. K. Jha, K. Prasad, *Int J Green Nanotech Phy Chem*. **2010**, *1*, 110–117.
- [42] T. K. Brito, R. L. S. Viana, C. J. G. Moreno, J. D. S. Barbosa, F. L. D. S. Júnior, M. J. C. de Medeiros, R. F. Melo-Silveira, J. Almeida-Lima, D. D. L. Pontes, M. S. Silva, et al. *Int. J. Nanomed*. **2020**, *15*, 965–979.
- [43] K. Chandhirasekar, A. Thendralmanikandan, P. Thangavelu, B. S. Nguyen, T. A. Nguyen, K. Sivashanmugan, A. Nareshkumar, V. H. Nguyen, *Mater. Lett*. **2020**, *287*, 129265.
- [44] B. Khodashenas, H. R. Ghorbanib, *Arab. J. Chem.y*. **2019**, *12*, 1823–1838.
- [45] K. Anandalakshmi, J. Venugobal, V. Ramasamy, *Appl Nanosci*. **2016**, *6*, 399–408.
- [46] A. G. Femi-Adepoju, A. O. Dada, K. O. Otun, A. O. Adepoju, O. P. Fatoba, *Heliyon*. **2019**, *23*, e01543.
- [47] S. M. Roopan, G. Rohit, Madhumitha, A. A. Rahuman, C. Kamaraj, A. Bharathi, T. V. Surendra, *Ind. Crops Prod*. **2013**, *43*, 631–635.
- [48] A. Rautela, J. Rani, M. Debnath Das, *J Anal Sci Technol*. **2019**, *10*, 5.
- [49] V. Kathiravan, S. Ravi, S. Ashokkumar, S. Velmurugan, K. Elumalai, C. P. Khatiwada, *Spectrochim. Acta A Mol. Biomol. Spectrosc*. **2015**, *139*, 200–205.
- [50] P. Mishra, S. Sohrab, S. K. Mishra, *Futur J Pharm Sci*. **2021**, *7*, 65.
- [51] B. M. Abdallah, E. M. Ali, *ACS Omega*. **2021**, *6*, 8151–8162.
- [52] P. Sanjenbam, J. V. Gopal, K. Kannabiran, *J Mycol Med*. **2014**, *24*, 211–219.
- [53] E. M. Ali, B. M. Abdallah, *Nanomaterials*. **2020**, *10*, 422.
- [54] J. S. Choi, J. W. Lee, U. C. Shin, M. W. Lee, D. J. Kim, S. W. Kim, *Nanomaterials*. **2019**, *9*, 1512.
- [55] M. Jalal, M. A. Ansari, M. A. Alzohairy, S. G. Ali, H. M. Khan, A. Almatroudi, M. I. Siddiqui, *Int. J. Nanomed*. **2019**, *14*, 4667–4679.
- [56] S. Prabhu, S. E. K. Poulouse, *International Nano Letters*. **2012**, *2*, 32.
- [57] Sondi, B. Salopek-Sondi, *J. Colloid Interface Sci*. **2004**, *275*, 177–182.
- [58] P. D. Bragg, D. J. Rainnie, *Can. J. Microbiol*. **1974**, *20*, 883–889.
- [59] G. McDonnell, A. D. Russell, *Clin. Microbiol. Rev*. **1999**, *12*, 147–179.
- [60] K. J. Kim, W. S. Sung, B. K. Suh, S. K. Moon, J. S. Choi, J. G. Kim, D. G. Lee, *BioMetals*. **2009**, *22*, 235–242.
- [61] A. Dantas, A. Day, M. Ikeh, I. Kos, B. Achan, J. Quinn, *J. Biomolecules*. **2015**, *5*, 142–165.

Submitted: August 4, 2022

Accepted: November 29, 2022